condensed matter

MDPI

Article

Plasma-Assisted Nitrogen Doping of Langmuir–Blodgett Self-Assembled Graphene Films

Tijana Tomašević-Ilić [1], Nikola Škoro [1], Đorđe Jovanović [1], Nevena Puač [1] and Marko Spasenović [2,*]

[1] Institute of Physics Belgrade, University of Belgrade, Pregrevica 118, 11080 Belgrade, Serbia
[2] Center for Microelectronic Technologies, Institute of Chemistry, Technology and Metallurgy, University of Belgrade, Njegoševa 12, 11000 Belgrade, Serbia
* Correspondence: spasenovic@nanosys.ihtm.bg.ac.rs

Abstract: Graphene films prepared from solution and deposited by Langmuir–Blodgett self-assembly technique (LBSA) were treated with radio-frequency (13.56 MHz) nitrogen plasma in order to investigate the influence of the time of nitrogen plasma exposure on the work function, sheet resistance, and surface morphology of LBSA graphene films. Kelvin probe force microscopy and sheet resistance measurements confirm nitrogen functionalization of our films, with the Fermi level shifting in a direction that indicates binding to a pyridinic and/or pyrrolic site. Upon 1 min of nitrogen plasma exposure, the sheet resistance decreases and there is no obvious difference in film morphology. However, plasma exposure longer than 5 min leads to the removal of graphene flakes and degradation of graphene films, in turn, affecting the flake connectivity and increasing film resistance. We show that by changing the exposure time, we can control the work function and decrease sheet resistance, without affecting surface morphology. Controllability of the plasma technique has an advantage for graphene functionalization over conventional doping techniques such as chemical drop-casting. It allows for the controllable tuning of the work function, surface morphology, and sheet resistance of LBSA graphene films, which is substantial for applications in various optoelectronic devices.

Keywords: graphene; liquid phase exfoliation (LPE); Langmuir–Blodgett assembly; nitrogen doping; low-temperature plasma

Citation: Tomašević-Ilić, T.; Škoro, N.; Jovanović, Đ.; Puač, N.; Spasenović, M. Plasma-Assisted Nitrogen Doping of Langmuir–Blodgett Self-Assembled Graphene Films. *Condens. Matter* **2023**, *8*, 34. https://doi.org/10.3390/condmat8020034

Academic Editor: Antonio Bianconi

Received: 15 January 2023
Revised: 14 March 2023
Accepted: 26 March 2023
Published: 4 April 2023

1. Introduction

Liquid phase exfoliation (LPE) is one of the simplest and most cost-effective methods for producing large flake quantities in dispersions of a broad range of layered materials [1]. LPE makes use of solvent molecules whose penetration between layers of bulk material is induced by turbulent motion of the solution [2]. LPE followed by Langmuir–Blodgett self-assembly (LBSA) deposition enables the production of thin films with high substrate coverage [3], and it satisfies practical application demands. Graphene films produced by LBSA from LPE solutions have high transparency throughout the visible part of the spectrum, with more than 80% transmittance. However, the limiting factor for the application of LBSA films in optoelectronic devices is the high density of defects that causes high sheet resistance [4]. The application in optoelectronic devices of films obtained by self-organization of graphene flakes requires appropriate surface modification/functionalization, to adapt the electrical properties of the films to the requirements of the electronic industry. Chemical modification of graphene has been a widely used technique to tailor graphene properties. It involves doping and surface modification during the graphene/graphene film preparation process or afterward as a post-treatment of pristine graphene. Different dopants have been applied to LBSA films in order to modify their properties [4–7]. However, most of the applied methods lower sheet resistance without affecting transparency, but provide little control over the amount of doping.

The use of non-equilibrium plasma for surface treatment and functionalization was investigated and it proved to be a versatile tool for processing many types of materials

used in electronics [8]. Plasma reactors operating at low pressures are able to create chemically reactive volumes of homogeneous plasma at room temperature with properties that can be adjusted by changing the working gas, pressure, plasma power, etc. [9], and by tuning plasma chemistry processes at surfaces, driven by high-energy electrons and reactive heavy particles created in the plasma, surface properties can be modified as desired. Nitrogen-based plasmas (in pure nitrogen or nitrogen mixtures) are frequently used in treatment of textiles or seeds due to their ability to activate the surface of the treated samples in order to apply nanoparticles or microcapsules or to activate the germination process in seeds [10–12].

Doping with nitrogen plasma is one of the most promising methods to precisely tailor the electronic properties of graphene [13,14]. There are three main bonding configurations of nitrogen in graphene [15]. Nitrogen atoms can be implanted at a graphitic site (in the basal plane), when nitrogen directly substitutes a carbon atom, and to a pyridinic or a pyrrolic site (at graphene edges). Each nitrogen bonding configuration affects the local charge distribution and local density of states differently, leading to different electronic properties. However, experimental results and theoretical calculations for N-plasma doping of CVD graphene suggest that optimal process conditions are required to bind N to graphene without the formation of excessive plasma-generated defects that can destroy the structure of homogenous graphene films [16].

In this study, we examined the electronic properties of Langmuir–Blodgett self-assembled graphene films exposed to radio-frequency (RF) nitrogen plasma and investigated the influence of nitrogen plasma exposure time on the work function, sheet resistance, and surface morphology of LBSA graphene films. KPFM measurements indicate that our films show p-type behavior and that nitrogen binds to the edges of graphene flakes in our LBSA films. AFM indicates that the morphology of our films strongly depends on the exposition time, and resistance measurements show that we can decrease sheet resistance by tuning exposure time.

2. Results

The plasma spectrum recorded at treatment conditions is presented in Figure 1. In the wavelength range between 200 nm and 1000 nm, we identified emission bands of nitrogen molecules: first positive system (transition $B^3\Pi_g$–$A^3\Sigma^+{}_u$), second positive system (transition $C^3\Pi_u$–$B^3\Pi_g$), and nitrogen ions: first negative system (transition $B^2\Sigma^+{}_u$–$X^2\Sigma^+{}_g$) [17,18]. The emission in the region below 285 nm may originate from excited N_2 (fifth positive and/or Gaydon–Herman singlet systems) or NO bands formed due to small amounts of oxygen impurities. Lines of atomic nitrogen have not been observed. However, this is due to the fact that dissociative excitation of N_2 or electron excitation of N atoms are not favored processes in low-pressure RF plasmas in nitrogen. This results in absence of N lines in the spectrum in this type of discharge generally [19] On the other hand, it has been demonstrated that these types of non-equilibrium plasmas have many advantages when used for plasma functionalization over conventional doping techniques [13].

The presence, density, and nature of defects determine the suitability of graphene for doping and other chemical modifications that can be used to change the electronic structure. The density and type of defects in graphene can be deduced from Raman spectra [20,21]. The appearance of D and D′ modes in Raman spectra indicates the presence of defects, the ratio of the intensities of the D and G modes is used to estimate defect density, while the ratio of intensities of the D and D′ modes is used to deduce the nature of defects. Figure 2 shows a typical Raman spectrum of an LBSA graphene film with well-resolved D, G, and 2D bands. The ratio of intensities of the D and G modes of 0.64 confirms a high density of defects in LBSA graphene films. The ratio of intensities of the D and D′ modes can be used to determine the dominant defect type in graphene, such as topological defects, edges, vacancies, substitutional impurities, and sp3 defects. In our films, the ratio of intensities of the D and D′ modes is 5.20, indicating that edges are dominant defect sites, and, as such,

may be considered the main reaction centers that enable surface modification of our films by nitrogen plasma doping.

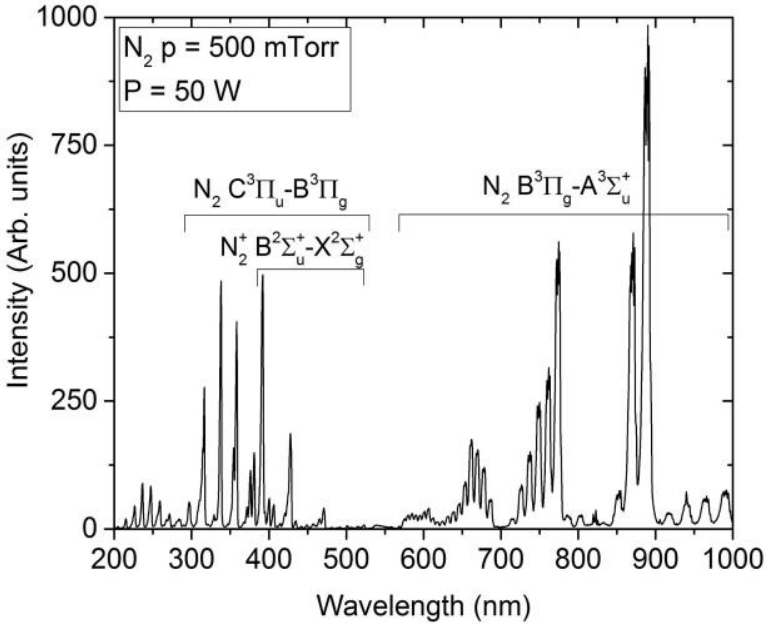

Figure 1. Emission spectrum of N_2 plasma with designation of the transition bands.

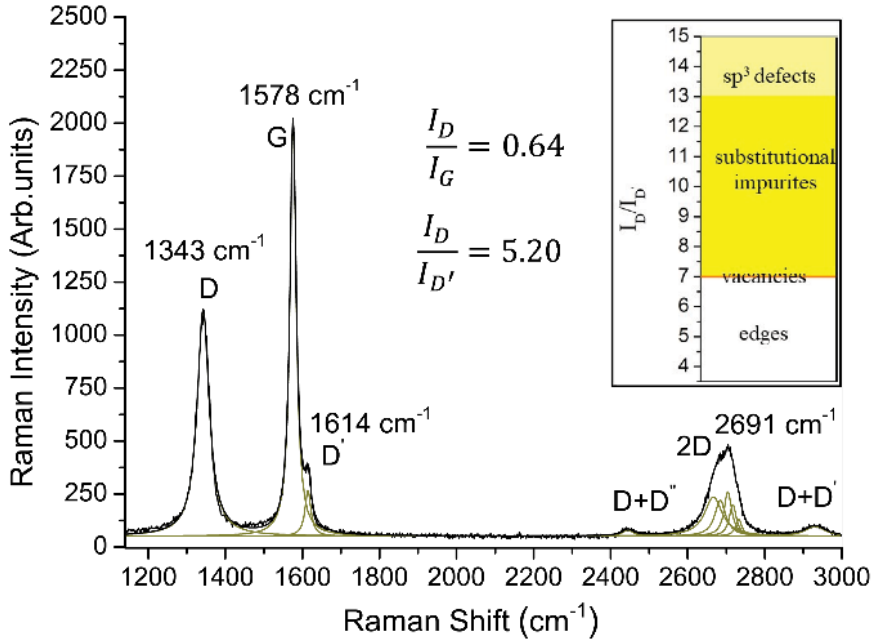

Figure 2. Representative Raman spectra of LBSA graphene film. Relationship between the value of the ratio between the intensity of the D and the D′ mode to the type of defect (inset) [20,21].

To examine the influence of nitrogen plasma doping on the electronic structure of LBSA films and predict the structural arrangement of nitrogen in doped LBSA films, we measured the surface work function (WF) of LBSA films with KPFM prior to and after nitrogen plasma treatment. Figure 3 depicts KPFM maps of the contact potential difference (CPD) between the sample and the tip before and after nitrogen exposure. Each of the surfaces shown on the different panels of Figure 3 has different CPD, as evidenced from the scale bars.

In order to determine the average CPD of the measured surface, histograms of corresponding KPFM maps (Figure 4a) were used. To measure the absolute value of the WF, we use as a reference the work function of highly ordered pyrolytic graphite (HOPG), a tabulated value of 4.6 eV. The work functions of the tip, HOPG, untreated, and treated films were related to their corresponding CPD measurements, as illustrated in Figure 4b. The work function of all graphene samples is larger than the reference value of 4.6 eV, indicating p-type behavior. It is found that nitrogen plasma treatment increases the WF from 4.89 eV to 5.1 eV, shifting the Fermi level downwards by ∼200 meV. Previous works already reported the strong correlation of the work function with the nitrogen doping site [22]. Since the work function is determined as the difference between the vacuum level and the Fermi level, a variation in the density of states near the Fermi level causes a change in the work function. In the case of graphitic nitrogen, nitrogen acts as an electron donor to the surrounding carbon atoms, inducing n-doping and a decrease in the work function. In the case of N binding to a pyridinic or a pyrrolic site, nitrogen acts as an electron acceptor resulting in the formation of a lone electron pair at the nitrogen atom and positively charged surrounding carbon atoms, inducing p-doping of graphene and an increase in the work function. Considering that nitrogen atoms bound to a graphitic site lower the work function, while nitrogen atoms at a pyridinic or a pyrrolic site increase the work function, from our KPFM measurements, we conclude that nitrogen binding to a pyridinic and/or pyrrolic site is dominant for LBSA graphene films. This is in agreement with the expected results for LBSA graphene films, where edges are the dominant defect type. Nitrogen binding to graphene is further confirmed with Fourier transform infrared spectroscopy (Figure S1, see Supplementary Information).

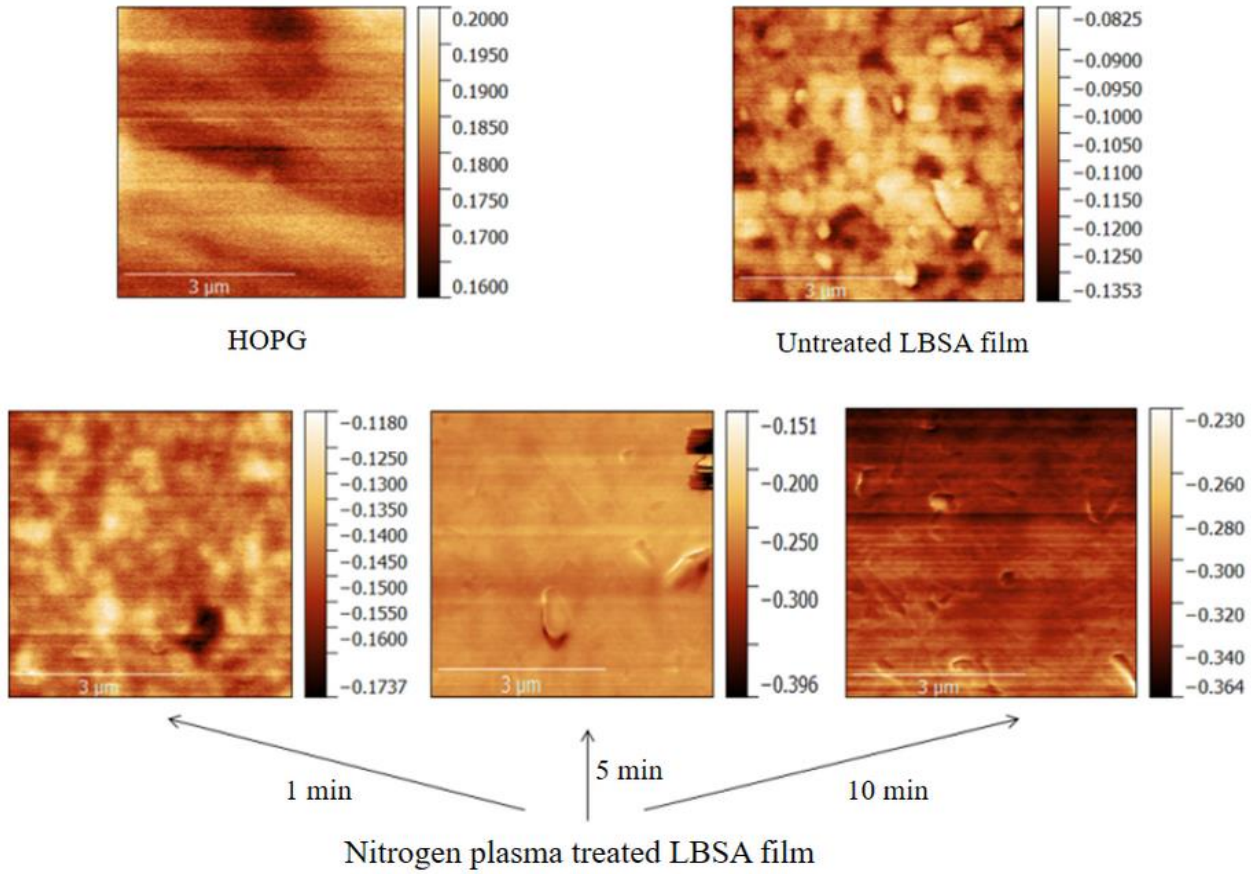

Figure 3. KPFM map of HOPG, untreated, and nitrogen-plasma-treated LBSA film for 1, 5, and 10 min nitrogen plasma exposure time.

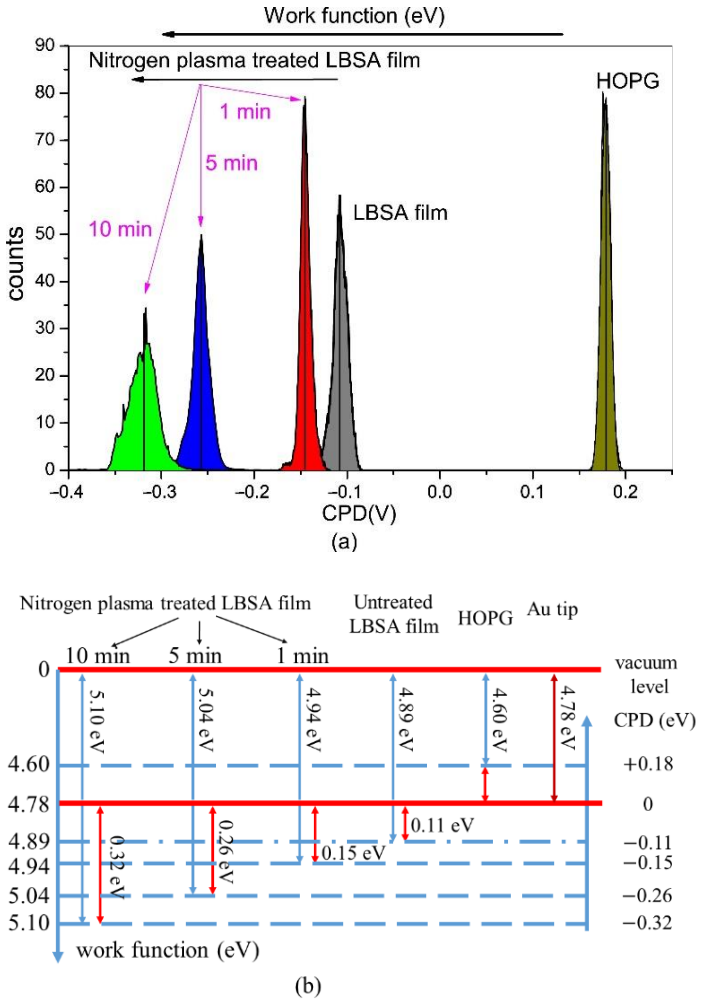

Figure 4. (**a**) KPFM histograms of LBSA graphene film before (gray) and after (red, blue, and green) doping, (**b**) schematic of the relationship between measured CPDs and their corresponding work functions.

Figure 5 depicts the sheet resistance of LBSA graphene films upon and after exposure to nitrogen plasma treatment. Prior to exposure, the sheet resistance of LBSA graphene is near 50 kΩ/sq. Upon 1 min of exposure, the sheet resistance decreases to around 45 kΩ/sq, remaining at a stable value as the exposure increases up to 5 min. Sheet resistance increases for exposure longer than 5 min. It appears that less than 5 min of exposure is enough for nitrogen doping to reach a saturation point. Further exposure of LBSA graphene films dramatically increases sheet resistance, leading to non-conductive films after 20 min of nitrogen plasma treatment.

To investigate the origins of the sheet resistance change with nitrogen plasma treatment, we examine the surface morphology of our films by AFM. Figure 6 depicts AFM topography of the same areas of the film that we used to measure the WF. AFM shows a high substrate coverage with broad lateral size and thickness distributions of overlapped graphene flakes. Compared with untreated LBSA graphene film, there is no obvious difference in film morphology after 1 or 5 min of exposure. However, there is a small change in film thickness after 5 min of treatment. Average film thickness is estimated as the peak-to-peak distance from histograms of sample/substrate edge areas before and after nitrogen exposure. The average thickness of our films is estimated as 5.2 nm for untreated, and 4.5 nm for 5 min nitrogen-plasma-treated LBSA films, indicating an average graphene sheet thickness of 17 and 15 layers, respectively (Figure 7). AFM measurements show that nitrogen plasma exposure longer than 5 min leads to the removal of graphene flakes,

and exposures of 10 and 20 min to the formation of voids and complete degradation of graphene films, in turn affecting flake connectivity, thereby increasing film resistance.

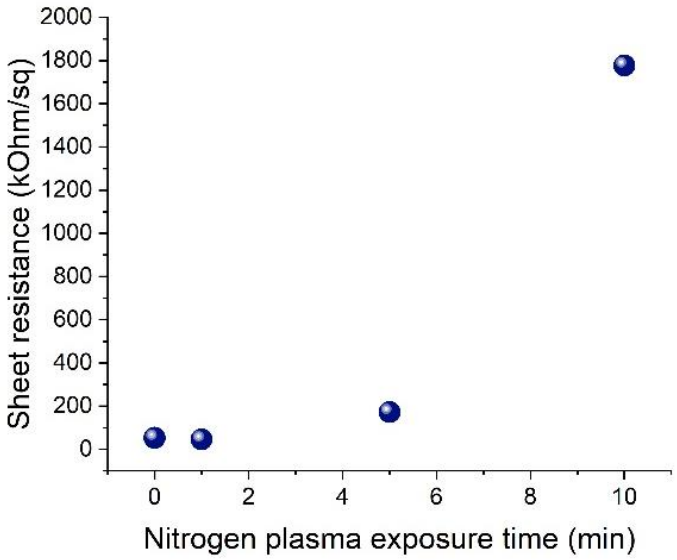

Figure 5. Sheet resistance of LBSA graphene films as a function of nitrogen plasma exposure time.

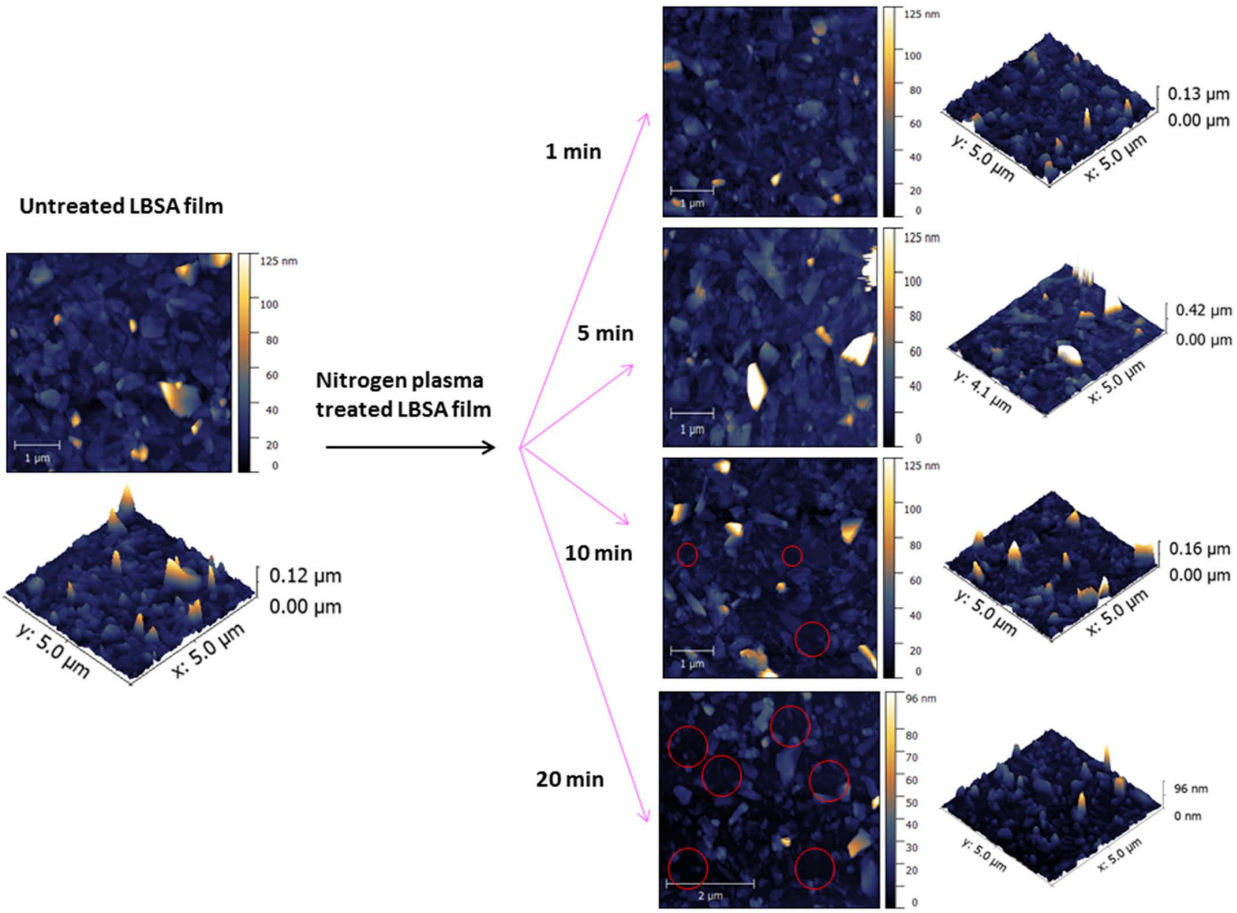

Figure 6. The 5 × 5 µm^2 topography of untreated, 1, 5, 10, and 20 min nitrogen-plasma-treated LBSA film and their corresponding 3D images. Red circles indicate the complete absence of graphene flakes.

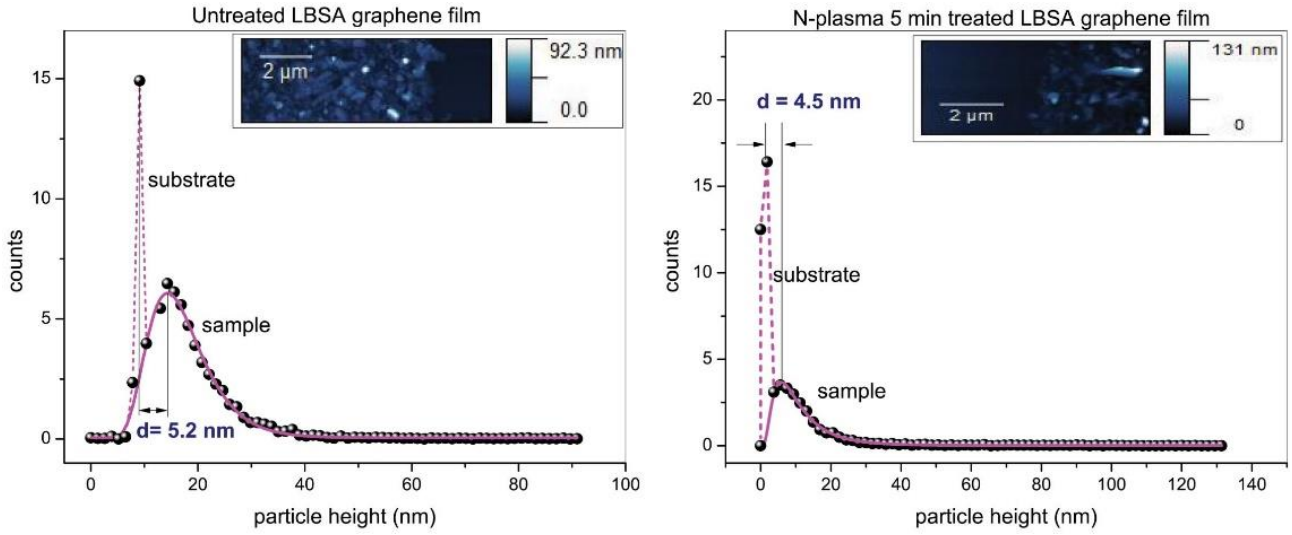

Figure 7. An untreated film/substrate (**left**) and 5 min treated film/substrate (**right**) height histogram obtained from AFM topography images (inset), and fitted by a log-normal curve (solid line).

For a further study of the processes occurring on the surface of the films and their stability, we performed vacuum annealing of the LBSA graphene films both before and after N plasma treatment. We have shown previously that untreated, as-made LBSA films undergo a decrease in resistance upon thermal treatment [6], which is also the case in this work. The sheet resistance decreases by a factor of ~2 upon annealing of pristine LBSA films. However, the films that are exposed to N plasma prior to annealing undergo a larger change in resistance upon annealing, as depicted in Figure 8. In fact, the longer a film is treated with plasma, the more its resistance changes during annealing. This effect is an indication that the described plasma treatment and doping of LBSA films is reversible with treatment, which can be useful for construction of practical sensor devices [23]. Plasma treatment reversibility with annealing is not surprising and has been observed in numerous studies before [24].

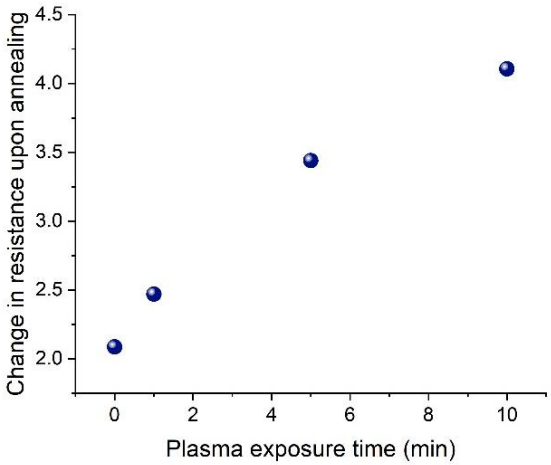

Figure 8. The effect of vacuum annealing on the sheet resistance of treated and untreated films.

3. Discussion

In this paper, we presented p-type doping of cost-effective and industrial-compatible LBSA graphene films with radio-frequency nitrogen plasma. KPFM measurements confirm the nitrogen functionalization of LBSA graphene films and an increase in the work function of all treated graphene samples indicates dominant binding to a pyridinic and pyrrolic site. KPFM measurements also show that the sensitivity of the work function to the time of the

nitrogen plasma exposure provides an opportunity to tune the work function of graphene thin films to the desired value. However, AFM and sheet resistance measurements indicate that more than 5 min of nitrogen plasma exposure degrades graphene films and increases sheet resistance. Although longer nitrogen plasma treatment affects the flake connectivity, the change in the exposure time could be used to adjust the work function up to 5.04 eV and to decrease sheet resistance without affecting surface morphology. Plasma treatment is shown to be an effective method of modifying the surface properties of graphene, which could be utilized for various purposes such as devices and coatings.

4. Materials and Methods

Graphene dispersions were produced from commercially available graphene powder (Sigma Aldrich, Taufkirchen, Germany) with the initial concentration of 18 mg/mL by liquid phase exfoliation in N-Methyl-2-pyrrolidone (NMP, Sigma Aldrich, Taufkirchen, Germany, product no. 328634) by the same procedure as previously reported [6,25]. The as-obtained dispersions were used for thin film formation by the Langmuir–Blodgett method. A small amount of the graphene dispersion was added to a water–air interface until the surface pressure became high enough to enable close-packing of graphene flakes and the formation of a compact film. The formed film was slowly scooped onto a SiO_2/Si substrate.

Plasma treatments were performed in a chamber with plane-parallel electrode geometry with 5 cm electrode gap and N_2 as working gas. The upper electrode was powered with a 13.56 MHz signal while the lower electrode was grounded and served as a sample holder. Before measurements, the chamber was evacuated to low pressure of a few mTorr in order to minimize impurities in the working gas. During the treatments, the pressure was kept constant at 500 mTorr of N_2. The RF power was fixed at 50 W with a reflected power of 0 W. The tuning parameter in this work was treatment duration, as the graphene films were exposed to nitrogen plasma for 1, 5, 10, and 20 min.

Raman measurement was performed using a TriVista 557 S&I GmbH Micro Raman spectrometer (λ = 532 nm) (Teledyne Princeton Instruments, Trenton, NJ, USA) at room temperature. FTIR spectra were recorded with a Nicolet Nexus 470 FT-IR spectrometer (Thermo Fisher Scientific, Waltham, MA, USA) over a range of 400–4000 cm^{-1}. All films are deposited on a ZnSe substrate.

Work function measurements were performed with Kelvin probe force microscopy (KPFM, NTEGRA Spectra, Limerick, Ireland) prior to and after photochemical treatment of our graphene films and the surface morphology of obtained graphene thin films was characterized with an atomic force microscope (AFM, NTEGRA Spectra, Limerick, Ireland) in tapping mode. The resistance of graphene films was measured in a four-point probe configuration (van der Pauw geometry).

Vacuum annealing was performed in a vacuum furnace CY-A1200-4IT (Zhengzhou CY Scientific Instrument, Zhengzhou, China) at a temperature of 150 °C and a vacuum of 10^{-2} mbar for one hour.

5. Conclusions

Our work demonstrates an effective method for controlled doping of LBSA graphene films with nitrogen plasma exposure. The work function, surface morphology, and sheet resistance of LBSA films can be controllably tuned by exposure time, which could be useful for tuning the properties of optoelectronic devices.

Supplementary Materials: The following supporting information can be downloaded at: https://www.mdpi.com/article/10.3390/condmat8020034/s1, Figure S1: FTIR absorption spectra of (a) untreated (black), (b) 1 min (red), and (c) 5 min (blue) N-plasma-exposed LBSA graphene films. We indicate vibrational modes for hydroxyls (possible C-OH, COOH, and H_2O contributions) at 3000–3700 cm^{-1}, carbonyl (C=O) and carboxyl groups (COOH) at 1600–1750 cm^{-1}, sp2-hybridized (C=C) at 1600 cm^{-1}, the C–O stretches of the hydroxyl and alkoxy groups at 1285 cm^{-1} and 1020–1045 cm^{-1}, respectively, C-N at 1430 and 1187 cm^{-1}, pyrrolic N at 1134 cm^{-1}, and epoxides (C-O-C) near 900 cm^{-1} (References [4,26–30] are cited in the supplementary materials).

Author Contributions: Conceptualization, T.T.-I., N.P. and M.S.; data curation, T.T.-I., N.Š. and M.S.; formal analysis, T.T.-I. and N.Š.; funding acquisition, T.T.-I., N.P. and M.S.; investigation, T.T.-I., N.Š., Đ.J., N.P. and M.S.; methodology, T.T.-I. and N.Š.; project administration, N.P. and M.S.; resources, T.T.-I., N.Š., Đ.J., N.P. and M.S.; supervision, N.P. and M.S.; validation, T.T.-I., N.Š., Đ.J., N.P. and M.S.; visualization, T.T.-I. and M.S.; writing—original draft, T.T.-I., N.Š., N.P. and M.S.; writing—review and editing, T.T.-I., N.P. and M.S. All authors have read and agreed to the published version of the manuscript.

Funding: This research was funded by the Institute of Physics Belgrade and the Institute of Chemistry, Technology, and Metallurgy, through grants from the Ministry of Science, Technological Development and Innovation of the Republic of Serbia (grant numbers: IPB 451-03-47/2023-01/200024; ICTM 451-03-47/2023-01/200026).

Data Availability Statement: Data are available on request from the corresponding author.

Conflicts of Interest: The authors declare no conflict of interest.

References

1. Bernal, M.M.; Milano, D. Two-dimensional nanomaterials via liquid-phase exfoliation: Synthesis, properties and applications. In *Carbon Nanotechnology*; Milne, W.I., Cole, M., Eds.; One Central Press: Manchester, UK, 2014; pp. 159–185.
2. Witomska, S.; Leydecker, T.; Ciesielski, A.; Samorì, P. Production and Patterning of Liquid Phase–Exfoliated 2D, Sheets for Applications in Optoelectronics. *Adv. Funct. Mater.* **2019**, *29*, 1901126. [CrossRef]
3. Kim, H.K.; Mattevi, C.; Kim, H.J.; Mittal, A.; Mkhoyan, K.A.; Riman, R.E.; Chhowalla, M. Optoelectronic properties of graphene thin films deposited by a Langmuir–Blodgett assembly. *Nanoscale* **2013**, *5*, 12365–12374. [CrossRef] [PubMed]
4. Tomašević-Ilić, T.; Jovanović, Đ.; Popov, I.; Fandan, R.; Pedrós, J.; Spasenović, M.; Gajić, R. Reducing sheet resistance of self-assembled transparent graphene films by defect patching and doping with UV/ozone treatment. *Appl. Surf. Sci.* **2018**, *458*, 446–453. [CrossRef]
5. Matković, A.; Milošević, I.; Milićević, M.; Tomašević-Ilić, T.; Pešić, J.; Musić, M.; Spasenović, M.; Jovanović, D.; Vasić, B.; Deeks, C. Enhanced sheet conductivity of Langmuir-Blodgett assembled graphene thin films by chemical doping. *2D Mater.* **2016**, *3*, 015002. [CrossRef]
6. Tomašević-Ilić, T.; Pešić, J.; Milošević, I.; Vujin, J.; Matković, A.; Spasenović, M.; Gajić, R. Transparent and conductive films from liquid phase exfoliated graphene. *Opt. Quant. Electron.* **2016**, *48*, 319. [CrossRef]
7. Milošević, I.R.; Vasić, B.; Matković, A.; Vujin, J.; Aškrabić, S.; Kratzer, M.C.; Griesser, T.; Teichert, C.; Gajić, R. Single-step fabrication and work function engineering of Langmuir-Blodgett assembled few-layer graphene films with Li and Au salts. *Sci. Rep.* **2020**, *10*, 8476. [CrossRef]
8. Makabe, T.; Petrović, Z.L. *Plasma Electronics*; Taylor and Francis: New York, NY, USA, 2006.
9. Škoro, N.; Puač, N.; Lazović, S.; Cvelbar, U.; Kokkoris, G.; Gogolides, E. Characterization and global modeling of low-pressure hydrogen-based RF plasmas suitable for surface cleaning processes. *J. Phys. D Appl. Phys.* **2013**, *46*, 475206. [CrossRef]
10. Gorenšek, M.; Gorjanc, M.; Bukošek, V.; Kovač, J.; Petrović, Z.; Puač, N. Functionalization of Polyester Fabric by Ar/N_2 Plasma and Silver. *Text. Res. J.* **2010**, *80*, 1633–1642. [CrossRef]
11. Kert, M.; Tavčer, P.F.; Hladnik, A.; Spasić, K.; Puač, N.; Petrović, Z.L.; Gorjanc, M. Application of Fragrance Microcapsules onto Cotton Fabric after Treatment with Oxygen and Nitrogen Plasma. *Coatings* **2021**, *11*, 1181. [CrossRef]
12. Živković, S.; Puač, N.; Giba, Z.; Grubišić, D.; Petrović, Z.L. The stimulatory effect of non-equilibrium (low temperature) air plasma pretreatment on light-induced germination of Paulownia tomentosa seeds. *Seed Sci. Technol.* **2004**, *32*, 693–701. [CrossRef]
13. Day, A.; Chroneos, A.; Braithwaite, N.S.J.; Gandhiraman, R.P.; Krishnamurthy, S. Plasma engineering of graphene. *Appl. Phys. Rew.* **2016**, *3*, 021301. [CrossRef]
14. Zeng, J.-J.; Lin, Y.-J. Tuning the work function of graphene by nitrogen plasma treatment with different radio-frequency powers. *Appl. Phys. Lett.* **2014**, *104*, 233103.
15. Granzier-Nakajima, T.; Fujisawa, K.; Anil, V.; Terrones, M.; Yeh, Y.T. Controlling Nitrogen Doping in Graphene with Atomic Precision: Synthesis and Characterization. *Nanomaterials* **2019**, *9*, 425. [CrossRef]
16. Yanilmaz, A.; Tomak, A.; Akbali, B.; Bacaksiz, C.; Ozceri, E.; Ari, O.; Senger, R.T.; Selamet, Y.; Zareie, H.M. Nitrogen doping for facile and effective modification of graphene surfaces. *RSC Adv.* **2017**, *7*, 28383–28392. [CrossRef]
17. Pearse, R.W.B.; Gaydon, A.G. *The Identification of Molecular Spectra*; Chapman and Hall Ltd.: London, UK, 1963.
18. Lofthus, A.; Krupenie, P.H. The spectrum of molecular nitrogen. *J. Phys. Chem. Ref. Data* **1977**, *6*, 113. [CrossRef]
19. Mansuroglu, D. Capacitively coupled radio frequency nitrogen plasma generated at two different exciting frequencies of 13.56 MHz and 40 MHz analyzed using Langmuir probe along with optical emission spectroscopy. *AIP Adv.* **2019**, *9*, 055205. [CrossRef]
20. Eckmann, A.; Felten, A.; Mishchenko, A.; Britnell, L.; Krupke, R.; Novoselov, K.S.; Casiraghi, C. Probing the nature of defects in graphene by raman spectroscopy. *Nano Lett.* **2012**, *12*, 3925–3930. [CrossRef]
21. Eckmann, A.; Felten, A.; Verzhbitskiy, I.; Davey, R.; Casiraghi, C. Raman study on defective graphene: Effect of the excitation energy, type, and amount of defects. *Phys. Rev. B* **2013**, *88*, 035426. [CrossRef]

22. Akada, K.; Terasava, T.; Imamura, G.; Obata, S.; Saiki, K. Control of work function of graphene by plasma assisted nitrogen doping. *Appl. Phys. Lett.* **2014**, *104*, 131602. [CrossRef]
23. Andrić, S.; Sarajlić, M.; Frantlović, M.; Jokić, I.; Vasiljević-Radović, D.; Spasenović, M. Carbon Dioxide Sensing with Langmuir–Blodgett Graphene Films. *Chemosensors* **2021**, *9*, 342. [CrossRef]
24. Yang, H.; Chen, M.; Zhou, H.; Qiu, C.; Hu, L.; Yu, F.; Chu, W.; Sun, S.; Sun, L. Preferential and Reversible Fluorination of Monolayer Graphene. *J. Phys. Chem. C* **2011**, *115*, 16844–16848. [CrossRef]
25. Andrić, S.; Tomašević-Ilić, T.; Rakočević, L.; Vasiljević-Radović, D.; Spasenović, M. Three Types of Films from Liquid-phase-exfoliated Graphene for Use as Humidity Sensors and Respiration Monitors. *Sens. Mater.* **2022**, *34*, 3933–3947. [CrossRef]
26. Acik, M.; Lee, G.; Mattevi, C.; Pirkle, A.; Wallace, R.M.; Chhowalla, M.; Cho, K.; Chabal, Y. The role of oxygen during thermal reduction of graphene oxide studied by infrared absorption spectroscopy. *J. Phys. Chem. C* **2011**, *115*, 19761–19781. [CrossRef]
27. Fedoseeva, Y.V.; Lobiak, E.V.; Shlyakhova, E.V.; Kovalenko, K.A.; Kuznetsova, V.R.; Vorfolomeeva, A.A.; Grebenkina, M.A.; Nishchakova, A.D.; Makarova, A.A.; Bulusheva, L.G.; et al. Hydrothermal Activation of Porous Nitrogen-Doped Carbon Materials for Electrochemical Capacitors and Sodium-Ion Batteries. *Nanomaterials* **2020**, *10*, 2163. [CrossRef]
28. Lazar, P.; Mach, R.; Otyepka, M. Spectroscopic Fingerprints of Graphitic, Pyrrolic, Pyridinic, and Chemisorbed Nitrogen in N-Doped Graphene. *J. Phys. Chem. C* **2019**, *123*, 10695–10702. [CrossRef]
29. Sudhakar, S.; Jaiswal, K.K.; Peera, G.; Ramaswamy, A.P. Green Synthesis of N-Graphene By Hydrothermal-Microwave Irradiation For Alkaline Fuel Cell Application. *Int. J. Recent Sci. Res.* **2017**, *8*, 19049–19053.
30. Kumar, M.P.; Kesavan, T.; Kalita, G.; Ragupathy, P.; Narayanan, T.N.; Pattanayak, D.K. On the large capacitance of nitrogen doped graphene derived by a facile route. *RSC Adv.* **2014**, *4*, 38689–38697. [CrossRef]